# Electron density at the Ag(110) surface studied by He diffraction

M. G. Dondi,* S. Terreni, and F. Tommasini†
*Dipartimento di Fisica, Università di Genova, Via Dodecaneso 33, 16146 Genova, Italy*

U. Linke
*Institut für Grenzflächenforschung und Vakuumphysik, Kernforschungsanlage Jülich G.m.b.H, D-5170 Jülich, West Germany*

(Received 25 June 1987; revised manuscript received 8 December 1987)

High-resolution helium-diffraction measurements from the Ag(110) surface, taken with beam energies $E_0=17.8$ meV and $E_1=64.6$ meV, angles of incidence ranging between 20° and 80°, and along the $\langle 001\rangle$, $\langle 1\bar{1}0\rangle$, and $\langle 1\bar{1}1\rangle$ crystal directions, are presented. The scattering data allow a detailed description of the He-metal interaction energy. The unperturbed electron density of the metal surface, determined from the interaction energy by using the effective-medium theory, is found to be in disagreement with the overlapping of atomic densities. In agreement with Harris and Liebsch's calculations [J. Phys. C **15**, 2275 (1982); Surf. Sci. **123**, 355 (1982)], the corrugation amplitudes of the isodensity surface are found to decay much faster than predicted by the overlapping of atomic densities.

## INTRODUCTION

The scattering of He atoms from metal surfaces was recently studied by several experimental groups. Bound-state resonance measurements yield the energies of the He-metal bound states for Ag(110),[1] Cu(113), Cu(115), and Cu(117),[2] while diffraction measurements taken with various angles of incidence and beam energies from metal surfaces as Ag(110),[3] Ni(110),[4] and Cu(110) (Ref. 5) yield the slope and the structure of the He-metal repulsive wall.

On theoretical ground Lang and Nørskov[6] show that the He-jellium interaction energy $V(z)$ is quite accurately represented both in the repulsive and in the well bottom regions by

$$V(z)=\alpha n(z)+V^A(z)\ , \tag{1}$$

where $\alpha$ is the effective averaged value of the Esbjerg-Nørskov constant,[7] $n(z)$ is the jellium electron density, and $V^A(z)$ represents the extra-exchange-correlation energy due to the inhomogeneity of the electron gas. For a real metal, as far as the size of the He atom is neglected and Takada and Kohn's arguments[8] discussed in Sec. IV are overlooked, Eq. (1) is generalized as[6,9]

$$V(x,y,z)=\alpha n(x,y,z)+V^A(x,y,z)\ . \tag{2}$$

This could make He scattering a powerful tool for surface studies allowing the experimental determination of the unperturbed electron density $n(x,y,z)$. Nevertheless, a few doubts[8] and ambiguities[9] in the use of Eq. (2) still remain. For this reason and in view of a systematic use of He-beam scattering as a probe for the electron density of chemisorbed layers[10] we present the first step of a study intended to submit Eq. (2) to a severe test for the He-Ag(110) system. In this case the lateral average $V_{00}(z)$ of $V(x,y,z)$ is asked to account for five bound-state energy levels known, from previous measurements, with accuracy better than 20 $\mu$eV.[1] Moreover the diffraction patterns taken along the $\langle 001\rangle$ direction present peaks up to the fourth order, thus yielding a large amount of experimental information. Weak diffraction peaks are also measured along the $\langle 1\bar{1}0\rangle$ and $\langle 1\bar{1}1\rangle$ directions, which allow a complete determination of $V(x,y,z)$. In order to conclude the test, accurate self-consistent calculations are needed. These are not available at present, hence we safely write

$$V(x,y,z)=V^R(x,y,z)+V^A(x,y,z)\ , \tag{3}$$

leaving for the discussion below and for further work to establish whether $V^R(x,y,z)$ can be expressed as $\alpha n(x,y,z)$ or not.

In Sec. I the experimental method is presented and the results of the whole set of measurements are given. Section II deals with a parametrization of Eq. (3) allowing easy analysis of the experimental data. The term $V^A(x,y,z)$ is fully described by accounting for theoretical results,[11–13] while $V^R(x,y,z)$ is represented by the overlapping of pseudoatomic anisotropic terms containing four free parameters. As shown in Sec. III two parameters are determined by the bound-state energy levels and the other two by the present diffraction data. The results discussed in Sec. IV support both Eq. (2) and the theory by Harris and Liebsch[14,15] dealing with the He-metal Hartree-Fock energy. On the other hand, a strong disagreement between the electron density given by the experiment and that given by the overlapping of isotropic atomic densities emerges. The anticorrugating role of the periodic van der Waals energy is also discussed.

## I. EXPERIMENT

The experimental apparatus, fully described elsewhere,[16] allows in-plane diffraction measurements for a modulated supersonic He beam. Two beam energies are used, $E_0=17.8\pm0.3$ meV and $E_1=64.6\pm2.5$ meV. The angular divergency is 0.2° in both cases while the velocity spread full width at half maximum (FWHM) is 1% and 4%, respectively. The crystal holder allows us to select

 

the angle of incidence $\theta_i$, to set the surface perpendicular to the plane containing the beam and the detector (scattering plane), and to rotate the surface around its normal. The rotatable detector, a differentially pumped quadrupole mass spectrometer designed in order to accept the whole direct beam, is seen from the surface as a circular aperture with full angular divergency of 0.7°. The Ag(110) surface is cleaned by a few cycles of ion bombardment followed by annealing at 450 °C and oxygen exposure.[17] During the measurements the crystal is held at the temperature $T_s = 135$ K. The surface contamination by the background gases makes the diffracted intensities decay by less than 5% in 10 h.

The He diffraction patterns, taken at $\theta_i = 30°$ and for different azimuthal directions, are shown in Fig. 1, where the ratio of the detected intensity $I$ to the intensity $I_0$ of the direct beam is plotted versus the scattering angle $\theta_f$. Figure 1(a) shows that strong diffracted peaks are observed when the ⟨001⟩ direction is oriented in the scattering plane, i.e., when the parallel momentum of the incoming atoms is perpendicular to the rows of close-packed Ag atoms. Along ⟨1$\bar{1}$0⟩ and ⟨1$\bar{1}$1⟩ weak diffraction peaks are observed, as shown in Figs. 1(b) and 1(c), respectively. For this reason most of the measurements are carried out along the ⟨001⟩ direction. For each diffraction peak the ratio

$$P_{mn}^{\text{expt}}(T_s) = \frac{I_{mn}\Delta\theta_{mn}}{I_0\Delta\theta_{00}} \tag{4}$$

is calculated. $I_{mn}$ and $\Delta\theta_{mn}$ are, respectively, the intensity of the maximum and the angular width (FWHM) of the $(m,n)$ diffraction peak, $I_0$ is the intensity of the direct beam, while $\Delta\theta_{00} = 0.7°$ is the angular width of the specular peak. $\Delta\theta_{mn}$ is somewhat larger than $\Delta\theta_{00}$ and quite accurately agrees with the estimate made by accounting for the velocity spread, the apparatus geometry, and the diffraction order.

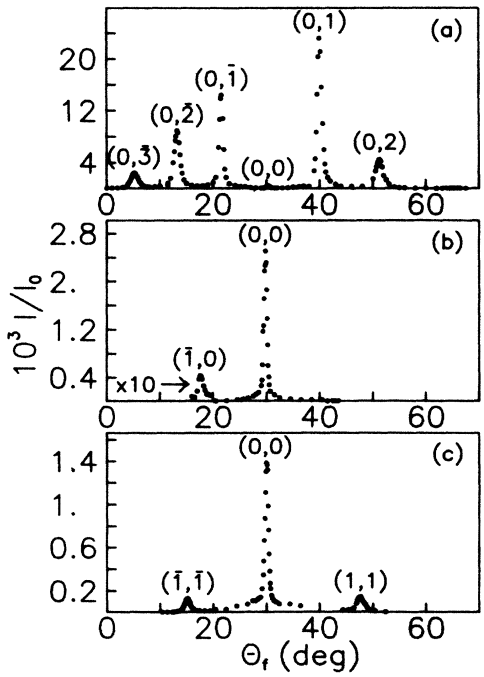


FIG. 1. He diffraction patterns measured with angle of incidence $\theta_i = 30°$ and beam energy $E_1 = 64.6$ meV for the azimuthal directions: (a) ⟨001⟩, (b) ⟨1$\bar{1}$0⟩, and (c) ⟨1$\bar{1}$1⟩.

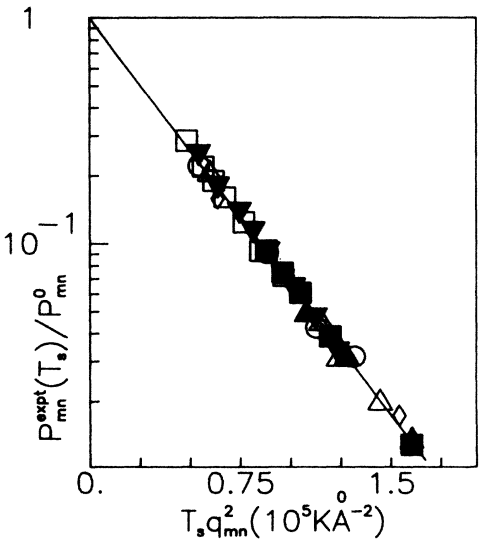


FIG. 2. Plot of the ratios $P_{mn}^{\text{expt}}(T_s)/P_{mn}^0$ vs $T_s q_{mn}^2$ obtained from the diffraction patterns measured along the ⟨001⟩ azimuth at angles of incidence $\theta_i = 20.5°$ and $\theta_i = 49.6°$. The beam energy is $E_1 = 64.6$ meV while the surface temperature ranges between 132 and 533 K. The diffraction peaks are labeled by ◇ (0,0), △ (0,1), ▲ (0,$\bar{1}$), ○ (0,2) for $\theta_i = 20.5°$ and by ▼ (0,0), □ (0,1), ■ (0,$\bar{1}$) for $\theta_i = 49.6°$.

Next, for a few angles of incidence, the thermally attenuated scattering ratios $P_{mn}^{\text{expt}}(T_s)$ are measured for several temperatures $T_s$ in the range from 135 to 500 K. The scattering ratios $P_{mn}^0$ which would be measured from an ideal static crystal, having even the zero-point motion frozen out, are obtained by the equation[18]

$$P_{mn}^{\text{expt}}(T_s) = P_{mn}^0 \exp(-cT_s q_{mn}^2) , \tag{5}$$

where $q_{mn}$ is the perpendicular momentum exchange, as obtained by including Beeby's correction,[19] and $c = 2.7\times10^{-5}$ Å$^2$K$^{-1}$ is a parameter, related to the surface Debye temperature,[18] obtained from the plot of the experimental results shown in Fig. 2. The whole set of scattering ratios $P_{mn}^0$ obtained from the measured diffraction patterns by using Eqs. (4) and (5) are given in Tables I–III.

## II. PARAMETRIZATION OF THE INTERACTION ENERGY

As shown in Fig. 3, the origin of the coordinates is chosen at a silver nucleus in the topmost layer, the $z$ axis is taken along the normal to the (110) surface, the $x$ axis along the ⟨1$\bar{1}$0⟩ crystal direction, and the $y$ axis along ⟨001⟩. $b = 2.880$ Å and $a = 4.073$ Å are the dimensions of the surface unit cell at the temperature $T_s = 135$ K,[20] while $\mathbf{G} \equiv \mathbf{G}_{mn} \equiv ((2\pi/b)m, (2\pi/a)n)$ are the unit vec-

TABLE I. Scattering ratios for several angles of incidence $\theta_i$, measured along the ⟨001⟩ direction with beam energy $E_0 = 64.6$ meV. The entries are $100P^0_{mn}$.

| | ⟨001⟩ | | | | | | |
|---|---|---|---|---|---|---|---|
| $\theta_i$(deg) \ $(m,n)$ | $(0,\bar{3})$ | $(0,\bar{2})$ | $(0,\bar{1})$ | (0,0) | (0,1) | (0,2) | (0,3) |
| 20.32 | | | 3.918 | 1.835 | 8.500 | 7.078 | 0.680 |
| 25.28 | | 8.262 | 5.838 | 0.703 | 10.51 | 5.448 | 0.280 |
| 30.26 | 2.869 | 8.128 | 8.924 | 0.162 | 12.52 | 3.525 | |
| 37.70 | 1.967 | 7.073 | 12.45 | 2.891 | 14.81 | 1.147 | |
| 45.22 | 1.183 | 5.954 | 15.19 | 11.04 | 10.48 | | |
| 50.20 | 0.762 | 4.383 | 15.75 | 20.69 | 6.48 | | |
| 55.42 | 0.374 | 2.735 | 13.84 | 33.28 | | | |
| 60.00 | 0.271 | 1.678 | 10.07 | 33.05 | | | |
| 65.07 | 0.130 | 1.005 | 7.345 | 46.69 | | | |
| 69.98 | 0.046 | 0.532 | 4.944 | 43.36 | | | |
| 75.21 | | 0.262 | 3.028 | 37.62 | | | |
| 79.91 | | 0.158 | 1.942 | 40.85 | | | |

TABLE II. Scattering ratios for several angles of incidence $\theta_i$, measured along the ⟨1$\bar{1}$1⟩ direction and the ⟨1$\bar{1}$0⟩ directions with beam energy $E_0 = 64.6$ meV. The entries are $100P^0_{mn}$.

| | ⟨1$\bar{1}$1⟩ | | |
|---|---|---|---|
| $\theta_i$(deg) \ $(m,n)$ | $(\bar{1},\bar{1})$ | (0,0) | (1,1) |
| 29.91 | 0.086 | 0.603 | 0.079 |
| 39.85 | 0.131 | 0.802 | 0.030 |
| 49.81 | 0.099 | 6.259 | |

| | ⟨1$\bar{1}$0⟩ | | |
|---|---|---|---|
| $\theta_i$(deg) \ $(m,n)$ | $(\bar{1},0)$ | (0,0) | (1,0) |
| 20.91 | 0.059 | 2.518 | 0.013 |
| 29.75 | 0.026 | 1.108 | |
| 35.00 | | 0.649 | |
| 40.00 | | 0.198 | |
| 45.00 | | 0.648 | |
| 50.00 | | 2.712 | |
| 55.00 | | 7.175 | |
| 60.00 | | 10.88 | |
| 65.00 | | 20.52 | |
| 70.00 | | 25.32 | |
| 75.00 | | 26.27 | |
| 80.00 | | 32.33 | |

TABLE III. Scattering ratios for several angles of incidence $\theta_i$, measured along the ⟨001⟩ direction with beam energy $E_0 = 17.8$ meV. The entries are $100P^0_{mn}$.

| | ⟨001⟩ | | | | |
|---|---|---|---|---|---|
| $\theta_i$(deg) \ $(m,n)$ | $(0,\bar{3})$ | $(0,\bar{2})$ | $(0,\bar{1})$ | (0,0) | (0,1) |
| 40.02 | 0.093 | 1.346 | 9.750 | 25.43 | 7.112 |
| 50.00 | | 1.158 | 8.454 | 27.58 | |
| 60.00 | | 0.770 | 6.878 | 29.29 | |
| 70.00 | | 0.501 | 5.822 | 39.38 | |
| 80.15 | | 0.307 | 3.763 | 23.49 | |

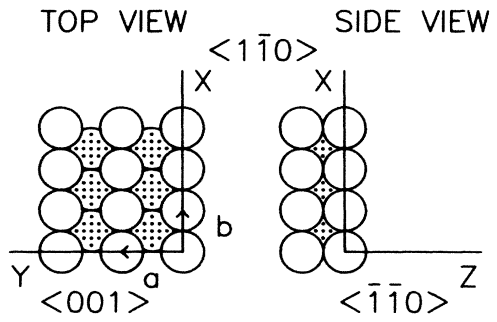


FIG. 3. Top and side view of the Ag(110) surface showing the choice of the reference system.

tors of the surface reciprocal lattice.

In order to describe analytically $V^R(x,y,z)$, using a set of free parameters which can be determined unambiguously from the experimental data, the overlapping of pseudoatomic anisotropic terms $v_j(x,y,z)$, extended to the silver sites in the topmost layer, is considered, i.e.,

$$V^R(x,y,z)=\sum_j v_j(x,y,z)\ ;$$
$$v_j(x,y,z)=\frac{A}{8\pi}\lambda_x\lambda_y\lambda_z\exp(-s_j)\ , \tag{6}$$

where

$$s_j=\{(\lambda_z z)^2+[\lambda_x(x-x_j)]^2+[\lambda_y(y-y_j)]^2\}^{1/2}\ . \tag{7}$$

As discussed in Sec. IV, for $\lambda_x=\lambda_y=\lambda_z=\lambda=2.42$ Å$^{-1}$, $V^R(x,y,z)$ in Eq. (6) is proportional to a true overlapping of atomic electron densities; in the present paper $\lambda_x$, $\lambda_y$, $\lambda_z$, and $A$ are considered as free parameters accounting phenomenologically for many-body effects in the surface environment. The interaction energy between He and the topmost layer is then written as the overlapping of pseudoatomic potentials with dispersion expansion limited to the leading term, i.e.,

$$V^I(x,y,z)=\sum_j\left[\frac{A}{8\pi}\lambda_x\lambda_y\lambda_z\exp(-s_j)-\frac{C_6}{r_j^6}f_6(s_j)\right]. \tag{8}$$

The function $f_6(s_j)$, damping the $C_6/r_j^6$ term, accounts for the overlapping of the He and Ag-pseudoatom electron clouds. It is conveniently written

$$f_n(\zeta)=1-\sum_{k=0}^{n}\frac{\zeta^k}{k!}\exp(-\zeta)\ , \tag{9}$$

as suggested by Tang and Toennies for the atom-atom case.[13] A lower limit for $C_6$ may be set according to Hill, Haller, and Celli.[12] These authors describe the van der Waals energy for the He–topmost-ion-core system by $\sum_j C_6/r_j^6$ with $C_6=4840$ meV Å$^6$. In the present case a somewhat larger $C_6$ is chosen in order to account for the $5s$ electrons.[21] This is done by requiring the term $V^A(x,y,z)$ in Eq. (2) or (3) to reproduce at long range Zaremba and Kohn's results,[11] given by

$$V^A(z)=-\frac{C}{(z-z_c)^3}\simeq-\frac{C}{z^3}-\frac{3z_cC}{z^4} \tag{10}$$

with $C=249$ meV Å$^3$ and $z_c=0.916$ Å.[22] By interpreting the term $3z_cC/z^4$ in Eq. (10) as the long-range lateral average of the term $\sum_j C_6 f_6(s_j)/r_j^6$ we set[22,23]

$$C_6=6abz_cC/\pi=5110\ \text{meV Å}^6\ . \tag{11}$$

The remaining term $C/z^3$ in Eq. (10), representing the contribution due to the crystal region extending from $z=-z_c$ to $z\to-\infty$, is then damped by $f_3(\lambda_z z)$ in order that

$$V^A(x,y,z)=-\sum_j\frac{C_6}{r_j^6}f_6(s_j)-\frac{C}{z^3}f_3(\lambda_z z) \tag{12}$$

vanish at the nuclear sites. In this way, at very short range, $V^R(x,y,z)$ in Eq. (3) represents the total interaction energy, in agreement with the effective-medium approximation.[6,9,24] At short range Eq. (12) should describe phenomenologically the extra-exchange-correlation energy due to the inhomogeneity of the electron gas, including part of the hybridization energy considered by Annett and Haydock.[25] The greatest part of this energy is possible accounted for by the first terms in the right-hand side of Eq. (1) (Ref. 25) or Eq. (2).[26]

In conclusion we assume that the full atom-surface potential $V(x,y,z)$ is represented by

$$V(x,y,z)=\sum_j\left[\frac{A}{8\pi}\lambda_x\lambda_y\lambda_z\exp(-s_j)-\frac{C_6}{r_j^6}f_6(s_j)\right]-\frac{C}{z^3}f_3(\lambda_z z)\ , \tag{13}$$

with $s_j$ given by Eq. (7), $f_n(\zeta)$ by Eq. (9), $C=249$ meV Å$^3$, $C_6=5110$ meV Å$^6$, and with $A$, $\lambda_x$, $\lambda_y$, and $\lambda_z$ free parameters. In further calculations Eq. (13) is substituted for by its lateral Fourier expansion

$$V(x,y,z)=\sum_{m,n}V_{mn}(z)\cos\left[\frac{2\pi}{b}mx\right]\cos\left[\frac{2\pi}{a}ny\right], \tag{14}$$

calculated numerically for each set of parameters. In Eq. (14) $m$ and $n$ are limited to non-negative integers.

## III. ANALYSIS OF THE EXPERIMENTAL DATA

Five bound states with the binding energies $\varepsilon_\nu^{\text{expt}}$ were recently observed by accurate bound-state resonance measurements.[1] The comparison of $\varepsilon_\nu^{\text{expt}}$ to the eigenvalues $\varepsilon_\nu^{\text{calc}}$ calculated exactly for the potential $V_{00}(z)$, lateral average of Eq. (13), is shown in Table IV. It should be noticed that the parameters $A=103.7$ eV Å$^3$ and $\lambda_z=2.78$ Å$^{-1}$ in Eq. (13) are determined by the bound-state data without substantial correlation with the parameters $\lambda_x$ and $\lambda_y$ which describe the surface corrugation. The values of $\lambda_x$ and $\lambda_y$ are then determined by fitting the diffraction probabilities $P_{mn}^{\text{calc}}$, calculated by the close-coupling method for $V(x,y,z)$, to $P_{mn}^0/(1-\beta)$. $P_{mn}^0$ are the scattering ratios reported in Tables I–III and $\beta$ is the

TABLE IV. Bound-state energy levels.

| $v$ | $-\varepsilon_v^{expt}$ (meV)[a] | $-\varepsilon_v^{calc}$ (meV)[b] |
|---|---|---|
| 0 | 4.44 ±0.02 | 4.440 |
| 1 | 2.18 ±0.02 | 2.179 |
| 2 | 0.92 ±0.02 | 0.921 |
| 3 | 0.31 ±0.02 | 0.326 |
| 4 | 0.095±0.015 | 0.089 |

[a]Experimental energy levels from Ref. 1.
[b]Energy levels calculated for the potential $V_{00}(z)$, lateral average of Eq. (13), with the parameters given in Eq. (15).

fraction of atoms lost for incoherent scattering due to the residual surface disorder. The values of the parameters yielding the results shown in Figs. 4–7 are $\beta=0.6$, $\lambda_x=2.02$ Å$^{-1}$, and $\lambda_y=2.17$ Å$^{-1}$. The quite good agreement reached for the whole set of experimental data strongly supports Eq. (13) and the set of parameters

$$A=103.7 \text{ eV Å}^3,\quad \lambda_x=2.02 \text{ Å}^{-1},\quad \lambda_y=2.17 \text{ Å}^{-1},\quad \lambda_x=2.78 \text{ Å}^{-1}. \tag{15}$$

The above values are determined with an accuracy better than 1%.

The convergency of the close-coupling calculations was checked by varying both the number of channels and the number of Fourier components of $V(x,y,z)$ accounted for. Only the $G_{mn}$ channels with $m<4$ and $n<6$ have to be retained and only the terms $V_{00}(z)$, $V_{01}(z)$, $V_{02}(z)$, $V_{10}(z)$, and $V_{11}(z)$ of the Fourier expansion of $V(x,y,z)$ significantly contribute to the calculated probabilities. The corresponding terms $V_{mn}^R(z)$ and $V_{mn}^A(z)$ are plotted in Figs. 8(a) and 8(b), respectively. In view of the following discussion it is useful to notice that all the terms, except $V_{00}^A(z)$, may be approximated, in the region of interest for He scattering, by the exponential functions

$$V_{mn}^R(z)=V_{mn}^R\exp(-\gamma_{mn}^R z);\quad V_{mn}^A(z)=V_{mn}^A\exp(-\gamma_{mn}^A z) \tag{16}$$

with the coefficients as reported in Table V.

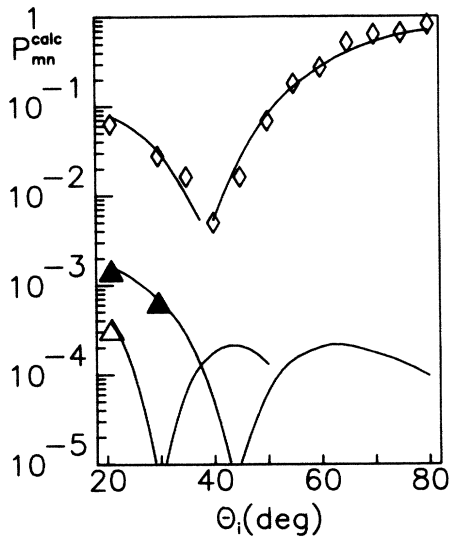


FIG. 5. Comparison of the calculated diffraction probabilities $P_{mn}^{calc}$ (solid lines) to the scattering ratios $P_{mn}^0$ measured along the $\langle 1\bar{1}0\rangle$ azimuth with beam energy $E_1=64.6$ meV. The diffraction peaks are labeled by ◇ (0,0), △ (0,1), ▲ (0,$\bar{1}$).

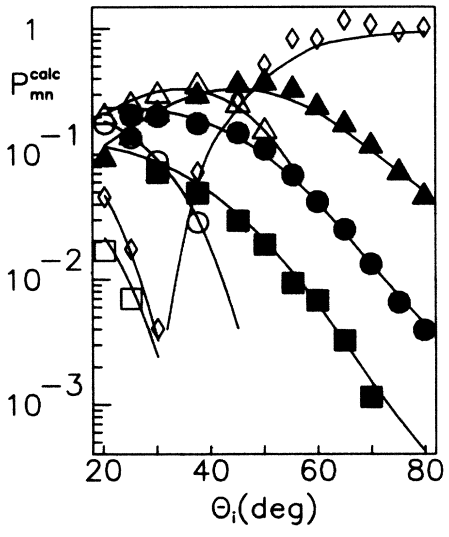


FIG. 4. Comparison of the calculated diffraction probabilities $P_{mn}^{calc}$ (solid lines) to the scattering ratios $P_{mn}^0$ measured along the $\langle 001\rangle$ azimuth with beam energy $E_1=64.6$ meV. The scattering ratios are divided by $1-\beta=0.4$. The diffraction peaks are labeled by ◇ (0,0), △ (0,1), ▲ (0,$\bar{1}$), ○ (0,2), ● (0,$\bar{2}$), □ (0,3), ■ (0,$\bar{3}$).

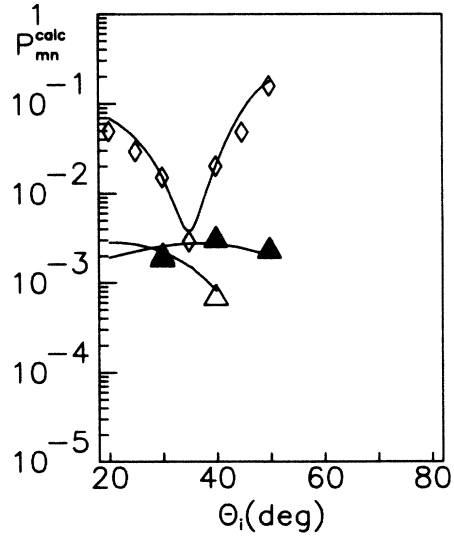


FIG. 6. Comparison of the calculated diffraction probabilities $P_{mn}^{calc}$ (solid lines) to the scattering ratios $P_{mn}^0$ measured along the $\langle 1\bar{1}1\rangle$ azimuth with beam energy $E_1=64.6$ meV. The scattering ratios are divided by $1-\beta=0.4$. The diffraction peaks are labeled by ◇ (0,0), △ (1,1), ▲ ($\bar{1}$,$\bar{1}$).

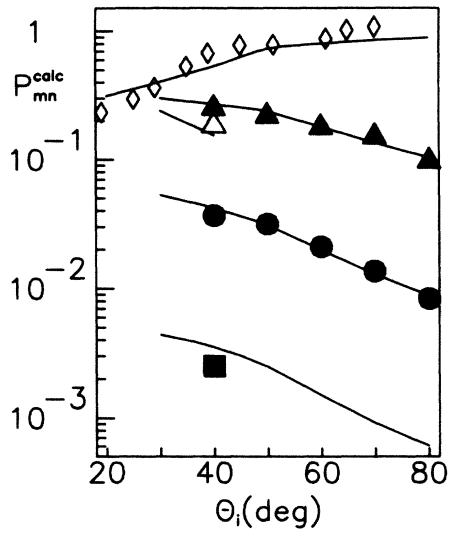


FIG. 7. Comparison of the calculated diffraction probabilities $P^{calc}_{mn}$ (solid lines) to the scattering ratios $P^0_{mn}$ measured along the ⟨001⟩ azimuth with beam energy $E_0=17.8$ meV. The scattering ratios are divided by $1-\beta=0.4$. The diffraction peaks are labeled by ◇ (0,0), △ (0,1), ▲ (0,$\bar{1}$), ● (0,$\bar{2}$), ■ (0,$\bar{3}$).

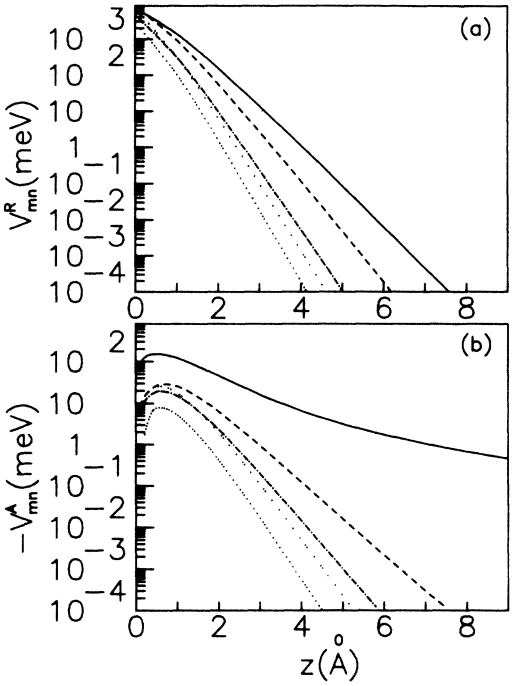


FIG. 8. (a) Lateral Fourier components of the repulsive potential $V^R$ defined in Eq. (6). ——, $V^R_{00}$; — — —, $V^R_{01}$; —·—·—·, $V^R_{10}$; · · · ·, $V^R_{11}$; · · ·, $V^R_{02}$. (b) Lateral Fourier components of the attractive potential $V^A$ defined in Eq. (12). ——, $V^A_{00}$; — — —, $V^A_{01}$; —·—·—·, $V^A_{10}$; · · · ·, $V^A_{11}$; · · ·, $V^A_{02}$.

## IV. DISCUSSION

Harris and Liebsch[14,15] (hereafter HL) show that the He-metal Hartree-Fock energy is proportional to $n(x,y,z)$ and that its Fourier components are approximated by exponential functions with decay constants $\gamma^{HL}_{mn}$ related to the work function $W$ and to the Fermi energy $E_F$ by simple equations.[14,27] As shown in Table V the HL decay constants calculated for Ag(110) with $W=4.52$ eV (Ref. 28) are in good agreement with the experimental results $\gamma^R_{mn}$. This does not necessarily mean that $V^R(x,y,z)=\alpha n(x,y,z)$. It cannot be excluded, in fact, that $V^R_{mn}(z)=\alpha_{mn}n_{mn}(z)$ with values of the proportionality constants $\alpha_{mn}$ depending on $m$ and $n$, as suggested by Takada and Kohn.[8] It seems more likely, however, that the discrepancies between calculations and experimental results referred to by Takada and Kohn arise from the representation of $n(x,y,z)$ as a true overlapping (hereafter TO) of atomic densities. In fact, when $n^{TO}(x,y,z)=\sum_j N\lambda^3\exp(-\lambda r_j)/(8\pi)$ is considered, the Fourier components $n^{TO}_{mn}(z)$, evaluated numerically, present decay constants $\gamma^{TO}_{mn}$ quite different from $\gamma^R_{mn}$ or $\gamma^{HL}_{mn}$ as shown in Table V. The failure of the TO is clearly evidenced by considering the decay constants of the corrugation amplitudes of the isodensity surfaces given by $\gamma^{TO}_{mn}-\gamma^{TO}_{00}$.[14,15,29] It appears that no choice of $\lambda$ allows one to obtain results in agreement with the experiment. Clearly, when only diffraction data taken along ⟨001⟩ are considered and no attempt to reproduce the bound-state spectrum is made, the TO may be led to agreement with the experiment by properly choosing $\lambda$. This, possibly, is the reason the TO successfully works in the Cu(110) case as proposed by Barker, Garcia, Batra, and Baumberger.[30] A second source of discrepancies between experiments and calculations arises when the periodic components of the van der Waals energy are neglected. These components play an important anticorrugating

TABLE V. (a) Parameters $V^A_{mn}$, $\gamma^A_{mn}$, $V^R_{mn}$, and $\gamma^R_{mn}$ in Eq. (16). (b) Decay constants $\gamma^{HL}_{mn}$ calculated according to Harris and Liebsch (Refs. 14, 15, and 28). (c) Decay constants $\gamma^{TO}_{mn}$ calculated for a true overlapping of atomic Herman-Skillman densities. $V$ values in eV, $\gamma$ values in Å$^{-1}$.

| | $(m,n)=$ | (0,0) | (0,1) | (1,0) | (1,1) | (0,2) |
|---|---|---|---|---|---|---|
| (a) | $V^A_{mn}$ | | −0.47 | −0.44 | −0.78 | −0.41 |
| | $\gamma^A_{mn}$ | | 2.06 | 2.56 | 2.97 | 3.37 |
| | $V^R_{mn}$ | 24.4 | 34.4 | 20.6 | 32.5 | 17. |
| | $\gamma^R_{mn}$ | 2.50 | 3.16 | 3.80 | 4.22 | 4.58 |
| (b) | $\gamma^{HL}_{mn}$ | 2.51 | 3.19 | 3.77 | 4.20 | 4.58 |
| (c) | $\gamma^{TO}_{mn}$ | 2.20 | 2.63 | 2.96 | 3.32 | 3.62 |

role, making $V_{mn}(z)$ substantially smaller than $V_{mn}^{R}(z)$ in the region where the turning points are located. This effect has increasing importance with higher-order G's due to the longer range of the van der Waals with respect to the repulsive interaction; as a consequence $V_{10}(z)$ becomes much smaller than $V_{01}(z)$ in the region of interest for He scattering and the diffraction patterns taken along $\langle 1\bar{1}0\rangle$ (and $\langle 1\bar{1}1\rangle$) present peaks smaller than can be expected by accounting only for the corrugation of the isoelectrondensity surfaces.

Firm conclusions on the above points can be drawn only when full self-consistent calculations of $n(x,y,z)$ to be compared with $V^{R}(x,y,z)$ are available; at present we tentatively conclude that Eq. (2) is correct, provided that $V^{A}(x,y,z)$ is described by Eq. (12), while the TO is in error. The overlapping method, extremely useful in order to represent $n(x,y,z)$ with a low number of parameters, is saved in the form

$$n(x,y,z)=\sum_j n_j(x,y,z)\ ;$$
$$n_j(x,y,z)=\frac{N_s}{8\pi}\lambda_x\lambda_y\lambda_z\exp(-s_j)\ , \tag{17}$$

where $n_j=v_j/\alpha$ and $N_s=A/\alpha$. The high anisotropy of $n_j(x,y,z)$ resulting from the set of parameters (15) suggests that strong many-body effects take place.

The charge density of a single silver atom, as calculated by using the Herman-Skillman tables of atomic orbitals,[31] is plotted for reference in Fig. 9 (dotted line). For $r>1.5$ Å it is approximated with percent accuracy by $N\lambda^3\exp(-\lambda r)/(8\pi)$ with $N=3.0$ and $\lambda=2.42$ Å$^{-1}$ (solid line), hence the free atom may be though of as consisting of a core with positive charge $eN$ surrounded by an isotropic electron cloud with containing $N=3$ effective electrons. The comparison of $\lambda_x,\lambda_y,\lambda_z$ with $\lambda$ shows that, with respect to the free-atom case, the electron density of the pseudoatom is compressed toward the surface and expanded in the surface plane mainly along the $\langle 1\bar{1}0\rangle$ azimuth. While the effective number of electrons $N_s$ for the surface pseudoatom could be at variance with $N$, the choice $N_s=N=3$ appears to be consistent with recent theoretical estimates of the Esbjerg-Nørskov constant. In fact, by setting $N_s=3$, the experiment leads to $\alpha=A/N_s=233$ eV$a_0^3$, in good agreement with $\alpha=\bar{\alpha}_{\rm eff}=255$ eV$a_0^3$ as given by Manninen, Nørskov, Puska, and Umrigar[9] and in even better agreement with $\alpha=\alpha_{-}=229$ eV$a_0^3$ as evaluated by Cole and Toigo.[24] The above discussion leads to a prescription for calculating $n(x,y,z)$ at a metal surface with given structure and work function. Get $N$ from the Herman-Skillman tables, set $N_s=N$, use the pseudo-overlapping in Eq. (17), and select $\lambda_x,\lambda_y,\lambda_z$ in order that the Fourier components $n_{mn}(z)$ decay as predicted by Harris and Liebsch.[14,15,27]

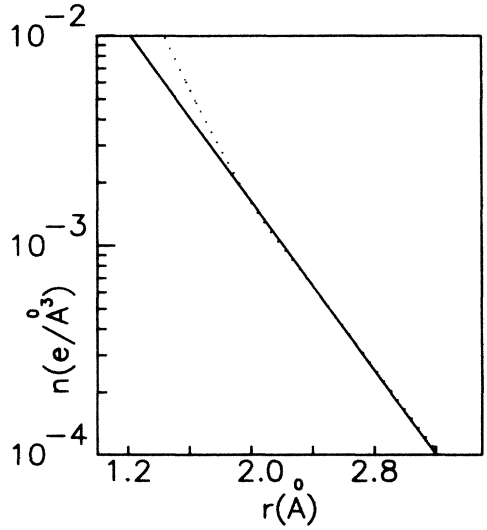


FIG. 9. Electron density of the free silver atom vs the distance from the nucleus as calculated by Herman and Skillman (Ref. 31) (dotted line). The solid line represents $N\lambda^3\exp(-\lambda r)/(8\pi)$ with $N=3.0$ and $\lambda=2.42$ Å$^{-1}$.

A comment on the damping of the van der Waals energy used in this paper is in order. We could have written Eq. (12) with the damping functions $f_6$ and $f_3$ substituted by $f_5$ and $f_2$, obtaining $V^{A}(x,y,z)$ proportional, at short range, to the electron density. Such an approach, possibly appropriate when the total interaction energy is split in the Hartree-Fock and van der Waals contributions as done by HL and by Nordlander and Harris,[32] was used in a previous paper dealing with the analysis of the bound-state spectrum.[1] In the present case $\alpha n(x,y,z)$ is expected to include the short-range van der Waals energy, hence the damping functions $f_6$ and $f_3$, together with a somewhat smaller $\alpha$ value, are used.

In conclusion, the main result of the present work consists in the determination of the interaction energy $V(x,y,z)$ for the system He-Ag(110) in the wide range $2<z<12$ Å; it is given by Eqs. (13) and (14) with $C_6=5110$ meV Å$^6$ and $C=249$ meV Å$^3$. It should be stressed that both the $C_6$ and $C$ values may be changed by $\pm 10\%$,[33,34] provided that $A$, $\lambda_x$, $\lambda_y$, and $\lambda_z$ are accordingly varied. Only $V(x,y,z)$ as a whole is out of the question; it is determined by the experiment with percent accuracy. Numerical calculations of $n(x,y,z)$ for Ag(110) having comparable accuracy in the region explored by the He atom would be very useful; when compared to $V(x,y,z)$ a complete calibration of the He-beam scattering method as a probe for the surface electron density could be achieved. After that a more refined analysis of the experimental results directed to the study of the short-range dispersion expansion[34] could be started.

## ACKNOWLEDGMENTS

Stimulating discussions with G. Boato, G. Bracco, P. Cantini, A. C. Levi, L. Mattera, C. Salvo, and R. Tatarek are gratefully acknowledged. This work was supported by Gruppo Nazionale di Struttura della Materia of the Consiglio Nazionale delle Ricerche (CNR) and by Centro Interuniversitario di Struttura della Materia of the Ministero della Pubblica Istruzione (MPI).

*Also at Istituto di Fisica della Facolta' di Ingegneria, Genova, Italy.

†Present address: Dipartimento di Fisica via A. Valerio 2, 34127 Trieste, Italy.

[1]M. G. Dondi, L. Mattera, S. Terreni, F. Tommasini, and U. Linke, Phys. Rev. B **34**, 5897 (1986).

[2]J. Perreau and J. Lapujoulade, Surf. Sci, **122**, 341 (1982).

[3]A. Luntz, L. Mattera, M. Rocca, S. Terreni, F. Tommasini, and U. Valbusa, Surf. Sci. **126**, 695 (1983).

[4]K. H. Rieder and W. Stocker, Phys. Rev. B **31**, 3392 (1985).

[5]B. Salanon, G. Armand, J. Perreau, and J. Lapujoulade, Surf. Sci. **127**, 135 (1983); D. Gorse, B. Salanon, F. Fabre, A. Kara, J. Perreau, G. Armand, and J. Lapujoulade, *ibid.* **147**, 611 (1984).

[6]N. D. Lang and J. K. Nørskov, Phys. Rev. B **27**, 4612 (1983).

[7]N. Esbjerg and J. Nørskov, Phys. Rev. Lett. **45**, 807 (1980).

[8]Y. Takada and W. Kohn, Phys. Rev. Lett. **54**, 470 (1985).

[9]M. Manninen, J. K. Nørskov, M. J. Puska, and C. Umrigar, Phys. Rev. B **29**, 2314 (1984), give an enlightening short discussion on the effective-medium theory.

[10]B. Buonopane, M. G. Dondi, S. Terreni, and F. Tommasini (unpublished).

[11]E. Zaremba and W. Kohn, Phys. Rev. B **13**, 2270 (1976).

[12]N. R. Hill, M. Haller, and V. Celli, Chem. Phys. **73**, 363 (1982).

[13]K. T. Tang and J. P. Toennies, J. Chem. Phys. **80**, 3726 (1984).

[14]J. Harris and A. Liebsch, J. Phys. C **15**, 2275 (1982); Surf. Sci. **123**, 355 (1982).

[15]A. Liebsch, J. Harris, B. Salanon, and J. Lapujoulade, Surf. Sci. **123**, 338 (1982).

[16]P. Chiaradia, M. G. Dondi, L. Mattera, C. Salvo, S. Terreni, and F. Tommasini (unpublished).

[17]The best results are obtained by forming and evaporating a $2\times1$ oxygen layer, G. Rovida and E. Zanazzi (private communication).

[18]G. Armand, J. Lapujoulade, Y. Lejay, Surf. Sci. **63**, 143 (1977).

[19]J. L. Beeby, J. Phys. C **4**, L359 (1971). The equation $q_{mn}=k\{[(\cos\theta_i)^2+D/E]^{1/2}+[(\cos\theta_{mn})^2+D/E]^{1/2}\}$, where $k$ is the beam wave vector, $D$ the well depth, and $E$ the beam energy, is used.

[20]W. B. Pearson, *Handbook of Lattice Spacings and Structures of Metals and Alloys* (Pergamon, Oxford, 1967), p. 499.

[21]A. M. Lahee, W. Allison, and R. F. Willis, Surf. Sci. **147**, L630 (1984).

[22]$z_c$ is given by $z_c=d/2+z_0$ where $d=b/2=1.44$ Å is the interlayer separation. The value $z_0=0.196$ Å is given in Ref. 11.

[23]W. A. Steele, *The Interaction of Gases with Solid Surfaces* (Pergamon, Oxford, 1974). For $z_0=0$, $z_c$ reduces to $b/2$ and Eq. (11) reduces to $C_6=6C/\pi N$ where $N$ is the bulk density of atoms.

[24]M. W. Cole and F. Toigo, Phys. Rev. B **31**, 727 (1985); **32**, 6989 (1985).

[25]J. F. Annett and R. Haydock, Phys. Rev. B **34**, 6860 (1986); Phys. Rev. Lett. **53**, 838 (1984).

[26]M. Karikorpi, M. Manninen, and C. Umrigar, Surf. Sci. **169**, 299 (1986).

[27]These are $\gamma_{mn}^{\mathrm{HL}}=[2m_e/\hbar^2(W+\Delta)]^{1/2}+[2m_e/\hbar^2(W+\Delta)+G_{mn}^2]^{1/2}$ where $\Delta\approx E_F/4$ is related to the Fermi energy $E_F$.

[28]A. W. Dweydary and C. H. B. Mee, Phys. Status Solidi A **27**, 223 (1975).

[29]Numerical calculations show that $\gamma_{mn}^{\mathrm{TO}}-\gamma_{00}^{\mathrm{TO}}\approx(\lambda^2+G_{mn}^2)^{1/2}-\lambda$.

[30]J. A. Barker, N. Garcia, I. P. Batra, and M. Baumberger, Surf. Sci. **141**, L317 (1984).

[31]F. Herman and S. Skillman, *Atomic Structure Calculations* (Prentice-Hall, Englewood Cliffs, New Jersey, 1963).

[32]P. Nordlander and J. Harris, J. Phys. C **17**, 1141 (1984).

[33]B. N. J. Persson and E. Zaremba, Phys. Rev. B **30**, 566 (1984).

[34]X. P. Jiang, F. Toigo, and M. W. Cole, Surf. Sci. **148**, 21 (1984).